

Green–Naghdi Theory, Part B: Green–Naghdi Equations for Deep Water Waves

Shiliang Duan¹, Binbin Zhao¹ and W. C. Webster²

Received: 03 December 2022 / Accepted: 12 December 2022
© The Author(s) 2023

Abstract

“Green–Naghdi Theory, Part A: Green–Naghdi (GN) Equations for Shallow Water Waves” have investigated the linear dispersion relations of high-level GN equations in shallow water. In this study, the GN equations for deep water waves are investigated. In the traditional GN equations for deep water waves, the velocity distribution assumption involves only one representative wave number. Herein, a new velocity distribution shape function with multiple representative wave numbers is employed. Further, we have derived the three-dimensional GN equations and analyzed the linear dispersion relations of the GN-3 and GN-5 equations. In this study, the finite difference method is used to simulate focus waves in the time domain. Additionally, the GN-5 equations are used to validate the wave profile and horizontal velocity distribution along water depth for different focused waves.

Keywords Green–Naghdi equations; Finite difference; Water waves; Deep water; Focused waves

1 Introduction

A growing number of studies are focusing on large-amplitude water waves because of their interesting strong nonlinearity property. Large waves in shallow water are strongly nonlinear and weakly dispersive. Moreover, large waves in deep water are extremely dispersive and nonlinear in nature. These deep water waves provide an important wave environment for ships and offshore platforms.

The Green–Naghdi (GN) theory is a significant nonlinear wave theory (Green et al. 1974; Green and Naghdi 1976). No small parameter is introduced in its derivation (Demirbilek and Webster 1992; Webster et al. 2011) except for velocity shape functions that vary with water

depth $\lambda_n(z)$. Many researches are using GN-1 (Level I GN) equations (Ertekin et al. 1986; Hayatdavoodi et al. 2019; Liu et al. 2019; Liu et al. 2020; Hayatdavoodi et al. 2022; Hayatdavoodi and Ertekin 2022; Kostikov et al. 2022). For shallow water waves, polynomials are used in the shape function in GN equations (Zhao et al. 2014; Wang et al. 2020). Zhao et al. (2014) applied high-level GN equations to wave transformation problems over the uneven seabed. Wang et al. (2020) studied the solitary wave in nonuniform shear currents using high-level GN equations with polynomial assumption.

In GN equations for deep water waves, exponentials are used for the shape functions. For example, Webster and Kim (1991) used $\lambda_n(z) = e^{k_n z} z^{n-1}$ as the shape function. However, only one representative wave number k was employed in their study. They used GN-3 (Level III GN) equations to simulate large-amplitude regular waves and long crest irregular waves in deep water. Zheng et al. (2016) investigated the problem of gravity wave group propagation with the GN equations involving traditional velocity assumption.

Webster and Zhao (2018) derived two-dimensional deep water GN equations using a novel velocity distribution function. This new velocity assumption utilized wave numbers, representing the form of $\lambda_n(z) = e^{k_n z}$. Further, Webster and Zhao (2018) studied the steady solution of the regular wave using the new deep-water GN equations. Their findings indicated that the new velocity assumption yields

Article Highlights

- To derive three-dimensional deep water GN equations using a new velocity assumption for future short-crest wave simulation.
- To apply the new deep water GN equations to water wave simulation in the time domain for the first time.
- To give the linear solution of new deep water GN equations.

✉ Zhao Binbin
zhaobinbin@hrbeu.edu.cn

¹ College of Shipbuilding Engineering, Harbin Engineering University, Harbin 150001, China

² Civil & Environmental Engineering, University of California, Berkeley CA94704, USA

more accurate results than the traditional velocity assumption, which has only one representative wave number.

Webster and Zhao (2018) investigated only steady-state solutions. Therefore, it is still unknown if the new deep water GN equations can be used to simulate deep water waves in the time domain. Therefore, this paper's motivations are 1) to derive three-dimensional deep water GN equations for future short-crest wave simulations using the new velocity assumption, 2) to apply the new deep water GN equations to time domain water wave simulation for the first time.

2 GN equations in deep water waves

We consider the free surface flow of an incompressible and inviscid fluid in infinite water depths. The coordinate system is chosen such that the z -axis points up and is directed against gravity, and the Oxy -plane is located on the free surface of still water. The location of the free surface is denoted by $z = \beta(x, y, t)$ and the bottom as $z = \alpha(x, y, t)$. It should be noted that the bottom is allowed to vary with time and space in the GN model.

We begin with the GN equations and the assumption of a general velocity distribution $\lambda_n(z)$.

$$\begin{cases} u(x, y, z, t) = u_0\lambda_0(z) + u_1\lambda_1(z) + u_2\lambda_2(z) + \dots + u_K\lambda_K(z) \\ v(x, y, z, t) = v_0\lambda_0(z) + v_1\lambda_1(z) + v_2\lambda_2(z) + \dots + v_K\lambda_K(z) \\ w(x, y, z, t) = w_0\lambda_0(z) + w_1\lambda_1(z) + w_2\lambda_2(z) + \dots + w_K\lambda_K(z) \end{cases} \quad (1)$$

The coefficients u_n , v_n , and w_n ($n = 0, 1, 2, \dots, K$) denote the unknown functions of (x, y, z, t) . K denotes the level of the GN theory. With these definitions, we obtain the following conditions.

The continuity condition:

$$\sum_{n=0}^K \left(\frac{\partial u_n}{\partial x} + \frac{\partial v_n}{\partial y} \right) \lambda_n(z) + \sum_{n=0}^K w_n \frac{d\lambda_n(z)}{dz} = 0 \quad (2)$$

The kinematic free surface and bottom conditions:

$$\frac{\partial \beta}{\partial t} = \sum_{n=0}^K \lambda_n(\beta) \left(w_n - \frac{\partial \beta}{\partial x} u_n - \frac{\partial \beta}{\partial y} v_n \right) \quad (3)$$

$$\frac{\partial \alpha}{\partial t} = \sum_{n=0}^K \lambda_n(\alpha) \left(w_n - \frac{\partial \alpha}{\partial x} u_n - \frac{\partial \alpha}{\partial y} v_n \right) \quad (4)$$

The three conservation equations of momentum:

$$E_n = \frac{1}{\rho} \left[-\frac{\partial P_n}{\partial x} + \hat{p}\lambda_n(\beta) \frac{\partial \beta}{\partial x} - \bar{p}\lambda_n(\alpha) \frac{\partial \alpha}{\partial x} \right] \quad (5)$$

$$F_n = \frac{1}{\rho} \left[-\frac{\partial P_n}{\partial y} + \hat{p}\lambda_n(\beta) \frac{\partial \beta}{\partial y} - \bar{p}\lambda_n(\alpha) \frac{\partial \alpha}{\partial y} \right] \quad (6)$$

$$G_n = \frac{1}{\rho} [P_n^* - \rho g S_n - \hat{p}\lambda_n(\beta) + \bar{p}\lambda_n(\alpha)] \quad (7)$$

for $n = 0, 1, 2, \dots, K$, where

$$E_n = \sum_{m=0}^K \left[\frac{\partial u_m}{\partial t} S_{mn} + \sum_{r=0}^K \left(\frac{\partial u_m}{\partial x} u_r + \frac{\partial u_m}{\partial y} v_r \right) S_{mrn} + \sum_{r=0}^K u_m w_r S_{rn}^m \right]$$

$$F_n = \sum_{m=0}^K \left[\frac{\partial v_m}{\partial t} S_{mn} + \sum_{r=0}^K \left(\frac{\partial v_m}{\partial x} u_r + \frac{\partial v_m}{\partial y} v_r \right) S_{mrn} + \sum_{r=0}^K v_m w_r S_{rn}^m \right]$$

$$G_n = \sum_{m=0}^K \left[\frac{\partial w_m}{\partial t} S_{mn} + \sum_{r=0}^K \left(\frac{\partial w_m}{\partial x} u_r + \frac{\partial w_m}{\partial y} v_r \right) S_{mrn} + \sum_{r=0}^K w_m w_r S_{rn}^m \right]$$

$$S_n = \int_{\alpha}^{\beta} \lambda_n dz, \quad P_n^* = \int_{\alpha}^{\beta} p \frac{d\lambda_n}{dz} dz,$$

$$S_{mn} = \int_{\alpha}^{\beta} \lambda_m \lambda_n dz, \quad S_{mrn} = \int_{\alpha}^{\beta} \lambda_m \lambda_r \lambda_n dz, \quad S_{rn}^m = \int_{\alpha}^{\beta} \frac{d\lambda_m}{dz} \lambda_r \lambda_n dz, \\ P_n = \int_{\alpha}^{\beta} p \lambda_n dz.$$

Equations (2), (3), (4), (5), (6), and (7) form the GN equations with general weight functions.

For shallow water problems, $1, z, z^2, \dots$, are frequently chosen as shape functions. For deep water waves, $e^{kz}, e^{kz}z, e^{kz}z^2, \dots$, are frequently chosen as shape functions where the parameter k is the single representative wave number. In this study, we employed a new velocity distribution assumption as described by Webster and Zhao (2018).

For deep water problems, we choose a new weighting function set given as:

$$\lambda_n(z) = e^{k_n z} \quad (8)$$

The velocity field is given by:

$$\begin{cases} u(x, y, z, t) = u_0 e^{k_0 z} + u_1 e^{k_1 z} + u_2 e^{k_2 z} + \dots + u_K e^{k_K z} \\ v(x, y, z, t) = v_0 e^{k_0 z} + v_1 e^{k_1 z} + v_2 e^{k_2 z} + \dots + v_K e^{k_K z} \\ w(x, y, z, t) = w_0 e^{k_0 z} + w_1 e^{k_1 z} + w_2 e^{k_2 z} + \dots + w_K e^{k_K z} \end{cases} \quad (9)$$

The equations for kinematic boundary conditions and conservations of mass and momentum can be reduced using Eq. (8). Hence, the free surface kinematic boundary conditions become:

$$\frac{\partial \beta}{\partial t} = \sum_{n=0}^K e^{k_n \beta} \left(w_n - \frac{\partial \beta}{\partial x} u_n - \frac{\partial \beta}{\partial y} v_n \right) \quad (10)$$

The bottom kinematic boundary conditions are satisfied at $z = \alpha(x, y, t) = -\infty$.

The continuity equation then becomes:

$$\sum_{n=0}^K \left(\frac{\partial u_n}{\partial x} + \frac{\partial v_n}{\partial y} \right) e^{k_n z} + \sum_{n=0}^K k_n w_n e^{k_n z} = 0 \quad (11)$$

If Eq. (11) is to hold everywhere, each coefficient must be set to zero, such that:

$$\frac{\partial u_n}{\partial x} + \frac{\partial v_n}{\partial y} + k_n w_n = 0 \quad (12)$$

Thus, the conditions for the conservation of momentum become:

$$E_n = \frac{1}{\rho} \left[-\frac{\partial p_n}{\partial x} + \hat{p} e^{k_n \beta} \frac{\partial \beta}{\partial x} \right] \quad (13)$$

$$F_n = \frac{1}{\rho} \left[-\frac{\partial p_n}{\partial y} + \hat{p} e^{k_n \beta} \frac{\partial \beta}{\partial y} \right] \quad (14)$$

$$G_n = \frac{1}{\rho} [P_n^* - \rho g S_n - \hat{p} e^{k_n \beta}] \quad (15)$$

for $n = 0, 1, 2, \dots, K$, where

$$\begin{aligned} E_n &= \sum_{m=0}^K \left[\frac{\partial u_m}{\partial t} S_{mn} + \sum_{r=0}^K \left(\frac{\partial u_m}{\partial x} u_r + \frac{\partial u_m}{\partial y} v_r \right) S_{mrn} + \sum_{r=0}^K u_m w_r S_{rm}^m \right] \\ F_n &= \sum_{m=0}^K \left[\frac{\partial v_m}{\partial t} S_{mn} + \sum_{r=0}^K \left(\frac{\partial v_m}{\partial x} u_r + \frac{\partial v_m}{\partial y} v_r \right) S_{mrn} + \sum_{r=0}^K v_m w_r S_{rm}^m \right] \\ G_n &= \sum_{m=0}^K \left[\frac{\partial w_m}{\partial t} S_{mn} + \sum_{r=0}^K \left(\frac{\partial w_m}{\partial x} u_r + \frac{\partial w_m}{\partial y} v_r \right) S_{mrn} + \sum_{r=0}^K w_m w_r S_{rm}^m \right] \end{aligned}$$

$$S_n = \int_{-\infty}^{\beta} e^{k_n z} dz, P_n^* = k_n \int_{-\infty}^{\beta} p e^{k_n z} dz$$

$$S_{mn} = \int_{-\infty}^{\beta} e^{(k_m + k_n)z} dz, S_{mrn} = \int_{-\infty}^{\beta} e^{(k_m + k_r + k_n)z} dz$$

$$S_{rm}^m = k_m \int_{-\infty}^{\beta} e^{(k_m + k_r + k_n)z} dz, P_n = \int_{-\infty}^{\beta} p e^{k_n z} dz$$

Note that:

$$P_n^* = k_n \int_{-\infty}^{\beta} p e^{k_n z} dz = k_n P_n \quad (16)$$

From Eq. (16), we can rewrite Eqs. (13), (14), and (16) as:

$$\frac{\partial P_n}{\partial x} = -\rho E_n + \hat{p} e^{k_n \beta} \frac{\partial \beta}{\partial x} \quad (17)$$

$$\frac{\partial P_n}{\partial y} = -\rho F_n + \hat{p} e^{k_n \beta} \frac{\partial \beta}{\partial y} \quad (18)$$

$$P_n = \frac{1}{k_n} (\rho G_n + \rho g S_n + \hat{p} e^{k_n \beta}) \quad (19)$$

By elimination and from Eqs. (17), (18), and (19), we obtain:

$$\frac{1}{k_n} \frac{\partial}{\partial x} (\rho G_n + \rho g S_n + \hat{p} e^{k_n \beta}) - \left(-\rho E_n + \hat{p} e^{k_n \beta} \frac{\partial \beta}{\partial x} \right) = 0 \quad (20)$$

$$\frac{1}{k_n} \frac{\partial}{\partial y} (\rho G_n + \rho g S_n + \hat{p} e^{k_n \beta}) - \left(-\rho F_n + \hat{p} e^{k_n \beta} \frac{\partial \beta}{\partial y} \right) = 0 \quad (21)$$

Eqs. (20) and (21) can be simplified to:

$$\frac{\partial}{\partial x} (G_n + g S_n) + k_n E_n + \frac{1}{\rho} \frac{\partial \hat{p}}{\partial x} e^{k_n \beta} = 0 \quad (22)$$

$$\frac{\partial}{\partial y} (G_n + g S_n) + k_n F_n + \frac{1}{\rho} \frac{\partial \hat{p}}{\partial y} e^{k_n \beta} = 0 \quad (23)$$

for $n = 0, 1, 2, \dots, K$.

For each K , a complete, closed set of equations is developed that is independent of all other K values. Thus, the kinematic models form a hierarchy depending on K and increase in complexity with K . However, this hierarchy is different from a perturbation expansion. Therefore, we adopted a terminology that describes the complexity of the theory. The GN equations in deep water with $K = 0$ and $K = 1$ are denoted as GN-1 (Level I) and GN-2 (Level II) equations, respectively.

3 Linear dispersion relations of GN equations

The linearized forms of the GN equations can be used to calculate the dispersion relation for a small amplitude linear sinusoidal wave.

For instance, in GN-3 ($K=2$) equations, we set the free surface pressure $\hat{p} = 0$. In the velocity assumption, we have $\lambda_n(z) = e^{k_n z}$ and used three representative wave numbers $k_0 = k_r/\gamma$, $k_1 = k_r$, $k_2 = k_r \gamma$, as suggested by Webster and Zhao (2018).

The linearized forms of GN-3 equations are:

$$\frac{\gamma u_{0,x}}{k_r} + \frac{u_{1,x}}{k_r} + \frac{u_{2,x}}{k_r \gamma} + \beta_{,x} = 0 \quad (24)$$

$$\begin{aligned} \frac{1}{2}u_{0,t} + \frac{k_r u_{1,t}}{\gamma \left(k_r + \frac{k_r}{\gamma}\right)} + \frac{k_r u_{2,t}}{\gamma \left(\frac{k_r}{\gamma} + \gamma k_r\right)} - \frac{\gamma^2 u_{0,xx}}{2k_r^2} \\ - \frac{u_{1,xx}}{k_r \left(k_r + \frac{k_r}{\gamma}\right)} - \frac{u_{2,xx}}{\gamma k_r \left(\frac{k_r}{\gamma} + \gamma k_r\right)} + g\beta_{,x} = 0 \end{aligned} \quad (25a)$$

$$\begin{aligned} \frac{k_r u_{0,t}}{k_r + \frac{k_r}{\gamma}} + \frac{1}{2}u_{1,t} + \frac{k_r u_{2,t}}{k_r + \gamma k_r} - \frac{\gamma u_{0,xx}}{k_r \left(k_r + \frac{k_r}{\gamma}\right)} - \frac{u_{1,xx}}{2k_r^2} \\ - \frac{u_{2,xx}}{\gamma k_r (k_r + \gamma k_r)} + g\beta_{,x} = 0 \end{aligned} \quad (25b)$$

$$\begin{aligned} \frac{\gamma k_r u_{0,t}}{\frac{k_r}{\gamma} + \gamma k_r} + \frac{\gamma k_r u_{1,t}}{k_r + \gamma k_r} + \frac{1}{2}u_{2,t} - \frac{\gamma u_{0,xx}}{k_r \left(\frac{k_r}{\gamma} + \gamma k_r\right)} - \\ \frac{u_{1,xx}}{k_r (k_r + \gamma k_r)} - \frac{u_{2,xx}}{2\gamma^2 k_r^2} + g\beta_{,x} = 0 \end{aligned} \quad (25c)$$

We assume that the free surface $\beta(x, t)$ and coefficient $u_0(x, t)$ can be expressed as:

$$\beta(x, t) = A \cos(kx - \omega t) \quad (26)$$

$$u_0(x, t) = \tilde{u}_0 \cos(kx - \omega t) \quad (27a)$$

$$u_1(x, t) = \tilde{u}_1 \cos(kx - \omega t) \quad (27b)$$

$$u_2(x, t) = \tilde{u}_2 \cos(kx - \omega t) \quad (27c)$$

Inserting Eqs. (26) and (27) into Eq. (25), we obtain:

$$\begin{aligned} \tilde{u}_0 = \frac{2Ag(1+\gamma)^2 k_r^2}{c(-1+\gamma)^2(k^2+k_r^2)} \\ \cdot \frac{(k^2-k_r^2)(k^2-\gamma^2 k_r^2)}{(k^4\gamma^2+k^2(1+\gamma(4+\gamma(2+\gamma)^2))k_r^2+\gamma^2 k_r^4)} \end{aligned} \quad (28a)$$

$$\begin{aligned} \tilde{u}_1 = \frac{2Ag(1+\gamma)^2}{c(-1+\gamma)^2(k^2+k_r^2)} \\ \cdot \frac{(-k^2+\gamma^2 k_r^2)(k^2\gamma^2 k_r^2-k_r^4)}{(k^4\gamma^2+k^2(1+\gamma(4+\gamma(2+\gamma)^2))k_r^2+\gamma^2 k_r^4)} \end{aligned} \quad (28b)$$

$$\begin{aligned} \tilde{u}_2 = \frac{2Ag\gamma^2(1+\gamma^2)}{c(-1+\gamma)^2(k^2+k_r^2)} \\ \cdot \frac{k_r^2(k^2-k_r^2)(k^2\gamma^2-k_r^2)}{(k^4\gamma^2+k^2(1+\gamma(4+\gamma(2+\gamma)^2))k_r^2+\gamma^2 k_r^4)} \end{aligned} \quad (28c)$$

Inserting Eqs. (26), (27) and (28) into Eq. (24), we can

obtain the linear dispersion relations of the GN-3 equations as:

$$\begin{aligned} c^2 = \frac{2gk_r}{(k^2+k_r^2)} \\ \cdot \frac{(k^4\gamma(1+\gamma+\gamma^2)+k^2(1+2\gamma+4\gamma^2+2\gamma^3+\gamma^4))k_r^2+\gamma(1+\gamma+\gamma^2)k_r^4}{(k^4\gamma^2+k^2(1+4\gamma+4\gamma^2+4\gamma^3+\gamma^4))k_r^2+\gamma^2 k_r^4} \end{aligned} \quad (29)$$

Next, we studied the dispersion relations of the GN-3 equations with $\gamma = 1.75$. For example, we select $k_r = 0.1$, and then employ the three representative wave numbers, $k_0 = k_r/\gamma = 0.057$, $k_1 = k_r = 0.1$ and $k_2 = k_r\gamma = 0.175$. Finally, the linear dispersion relations of the GN-3 equations with $\gamma = 1.75$ and $k_r = 0.1$ are shown in Figure 1.

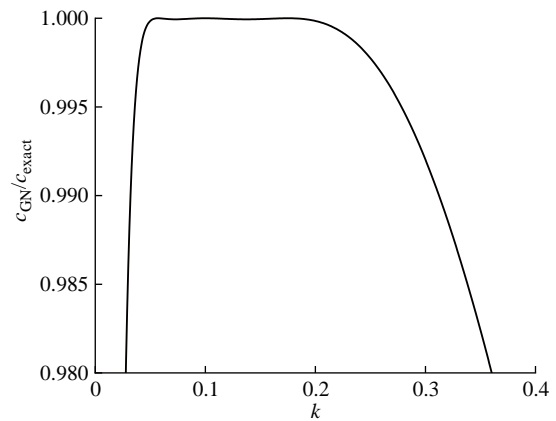


Figure 1 Dispersion relations of the GN-3 equations with $\gamma = 1.75$

Figure 1 shows the nondimensional wave celerity of the GN-3 equations, i.e., $c_{\text{GN}}/c_{\text{exact}}$, where c_{exact} denotes the exact linear wave celerity $c_{\text{exact}} = \sqrt{g/k}$. For waves whose wave numbers are in the range of $0.057 < k_r < 0.175$, i.e., waves whose wavelengths belong to $36 \text{ m} < \lambda < 110 \text{ m}$, the GN-3 equations with $\gamma = 1.75$ and $k_r = 0.1$ simulates the linear wave celerity accurately. $c_{\text{GN}}/c_{\text{exact}}$ is approximately 1 in that range. Hence, we could say that the GN-3 equations with $\gamma = 1.75$ and $k_r = 0.1$ can simulate a narrow wave spectrum with its peak energy located within $36 \text{ m} < \lambda < 110 \text{ m}$.

If we increase the parameter γ to 2.5, keeping all the other parameters constant and still selecting $k_r = 0.1$, then the three representative wave numbers would be $k_0 = k_r/\gamma = 0.04$, $k_1 = k_r = 0.1$, and $k_2 = k_r\gamma = 0.25$. The linear dispersion relations of the GN-3 equations with $\gamma = 2.5$ and $k_r = 0.1$ are shown in Figure 2.

Figure 2 shows that for waves whose wave numbers belong to $0.04 < k_r < 0.25$, i.e., waves whose wavelengths belong to $25 \text{ m} < \lambda < 157 \text{ m}$, the GN-3 equations with $\gamma = 2.5$ and $k_r = 0.1$ can simulate the linear wave celerity accu-

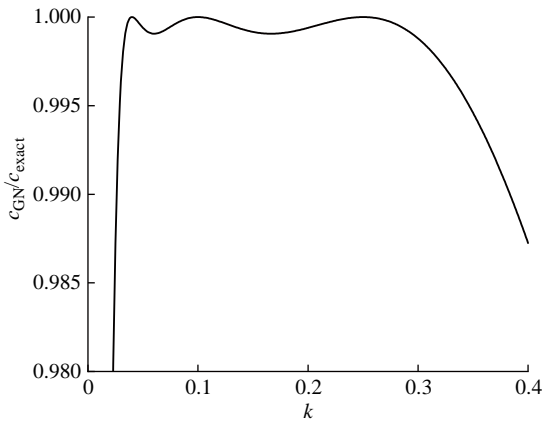


Figure 2 Dispersion relations of the GN-3 equations with $\gamma = 2.5$

rately. Moreover, since the wave celerity error is less than 0.1%, we can say that the GN-3 equations with $\gamma = 2.5$ and $k_r = 0.1$ can simulate a wider wave spectrum with main energy located in $25 \text{ m} < \lambda < 157 \text{ m}$.

If we further increase the parameter γ to 3.5, we can see from Figure 3 that the wave celerity error increases to 0.5% for waves whose wavenumbers belong to $0.029 < k_r < 0.35$, i.e., waves whose wavelengths belong to $18 \text{ m} < \lambda < 220 \text{ m}$. We discovered that the accuracy of the dispersion relations of the GN equations reduces when γ is too large, as shown in Figure 3.

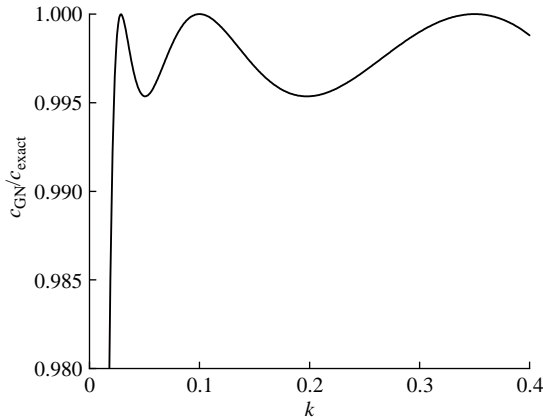


Figure 3 Dispersion relations of the GN-3 equations with $\gamma = 3.5$

Herein, we studied another parameter, that is, the level of the GN equations. Let us consider an increase in the level from GN-3 to GN-5, which is $K=4$. Then, in GN-5 equations, we employ five representative wave numbers: $k_0 = k_r/\gamma^2$, $k_1 = k_r/\gamma$, $k_2 = k_r$, $k_3 = k_r\gamma$, and $k_4 = k_r\gamma^2$. Using a similar derivation method, we can obtain the linear solution of GN-5 equations and their linear dispersion relations. Figure 4 shows the comparison between GN-3 and GN-5 dispersion relations with $k_r = 0.1$ and $\gamma = 2.5$.

From Figure 4, waves whose wavenumbers are in the range $0.016 < k_r < 0.625$, i.e., waves whose wavelengths

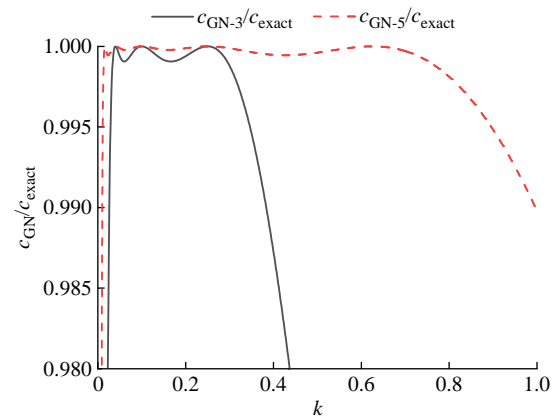


Figure 4 Comparison between the GN-3 and GN-5 dispersion relations

belong to $10 \text{ m} < \lambda < 393 \text{ m}$, the GN-5 equations with $\gamma = 2.5$ and $k_r = 0.1$ simulates them accurately. The wave celerity error calculated by GN-5 equations is less than 0.1%. We know from Figure 4 that GN-5 equations could simulate a much wider spectrum than GN-3 equations, where the wavelength range of $10 \text{ m} < \lambda < 393 \text{ m}$ covers most of the waves in the deep sea.

4 Numerical simulation of focused waves

The finite difference method is used to solve the new GN equations in the water wave time domain simulation; for more information on the numerical simulation algorithm (Zhao et al. 2014).

Baldock et al. (1996) conducted an experimental study in a wave flume on unidirectional focused waves. The study area was 20 m long, 0.3 m wide, and 0.7 m deep. In these experiments, 29 independent regular waves of varying frequencies were used in the wavemaker to generate a focused wave. Further, focused waves with amplitudes of 22 mm, 38 mm, and 55 mm were investigated. Each regular wave at the wave maker has the same amplitude as 22/29 mm, 38/29 mm, and 55/29 mm, respectively. The focal point of a series of regular waves of varying frequencies is expected to be at $x_f = 8.0 \text{ m}$ from linear wave theory. Cases B and D have different wave period ranges, as shown in Table 1.

Table 1 Focused wave input characteristics

Case name	Period range (s)
Case B	$0.6 \leq T_i \leq 1.4$
Case D	$0.8 \leq T_i \leq 1.2$

Through a time domain numerical simulation, the new deep water GN equations with infinite water depth are used to reproduce these focused waves for Cases B and D. The expected focal position of the numerical simulation is the same as that obtained from the experiment, which is

$x_f = 8.0$ m. Therefore, the focal time must be sufficient for the shortest regular wave component to pass through the theoretical focal position; that is $t_f \geq x_f/c_{g\min} = 15$ s, where $c_{g\min}$ is the group velocity of the shortest regular wave component. Thus, we choose $t_f = 20$ s as the focal time. The spatial and temporal resolutions (dx , dt) of the numerical simulation correlate with λ_{\min} and c_{\max} , respectively. λ_{\min} is the wavelength of the shortest regular wave component and c_{\max} is the phase velocity of the longest regular wave component. Through self-convergence tests, the spa-

tial and temporal resolutions are set as $dx = \lambda_{\min}/30$ and $dt = dx/(4c_{\max})$. The following results were obtained with the GN-5 equations with $\gamma = 1.75$ and $k_r = 5.0$. Figure 5 depicts the numerical results of the proposed new GN equations on wave elevation time histories at the focal position for Cases B and D.

The black line in Figure 5 represents the numerical results of new deep water GN equations, while the red circle represents the HLIGN results with a 2.1 m water depth, as reported by Zhao et al. (2020). For Cases B and D, Zhao

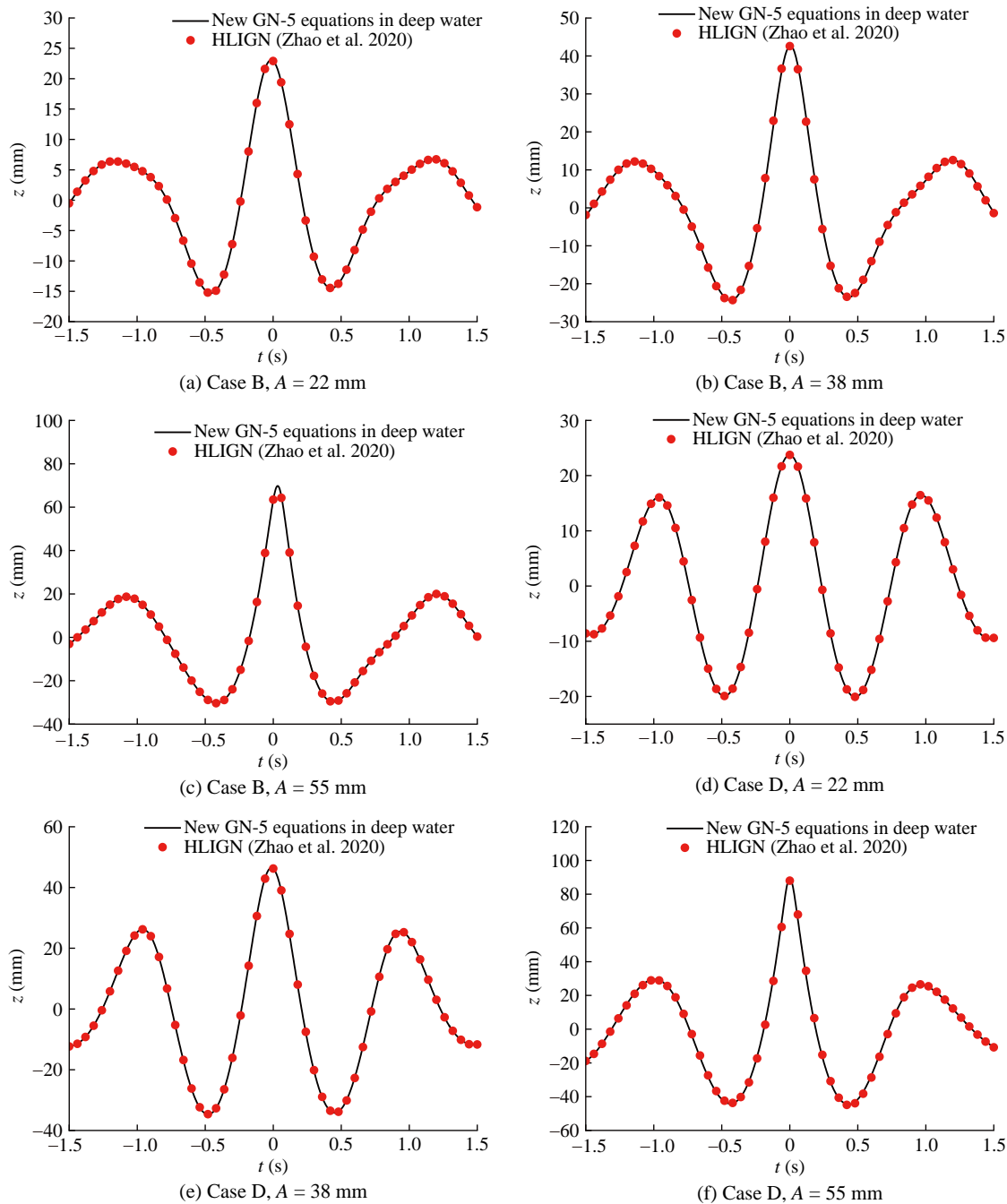


Figure 5 Time series at the focal position for Case B and Case D

et al. (2020) discovered that the wave flume experimental data (Baldock et al. 1996) with 0.7 m water depth are not deep water focus wave results. Therefore, Zhao et al. (2020) used the HLIGN equations based on polynomials as shape functions to calculate deep water focus waves at 2.1 m depth. As a result, rather than using the experimental data from Baldock et al. (1996), the HLIGN equation results from Zhao et al. (2020) are used to validate the present new deep water GN equations (infinite water depth). Hence, from Figure 5, it can be inferred that there is a good agreement on focus wave elevation between the

current results and results derived from the HLIGN equation with a 2.1 m water depth (Zhao et al. 2020).

Figure 6 depicts the horizontal velocity distribution along water depth beneath the focused crest of the new GN-5 deep water equations.

The black and red dashed lines in Figure 6 represent the numerical results of the new deep water GN equations and HLIGN equations with a 2.1 m water depth (Zhao et al. 2020). The horizontal velocity distribution along water depth under the focal point calculated by these two equations is in good agreement. The horizontal velocity at $z =$

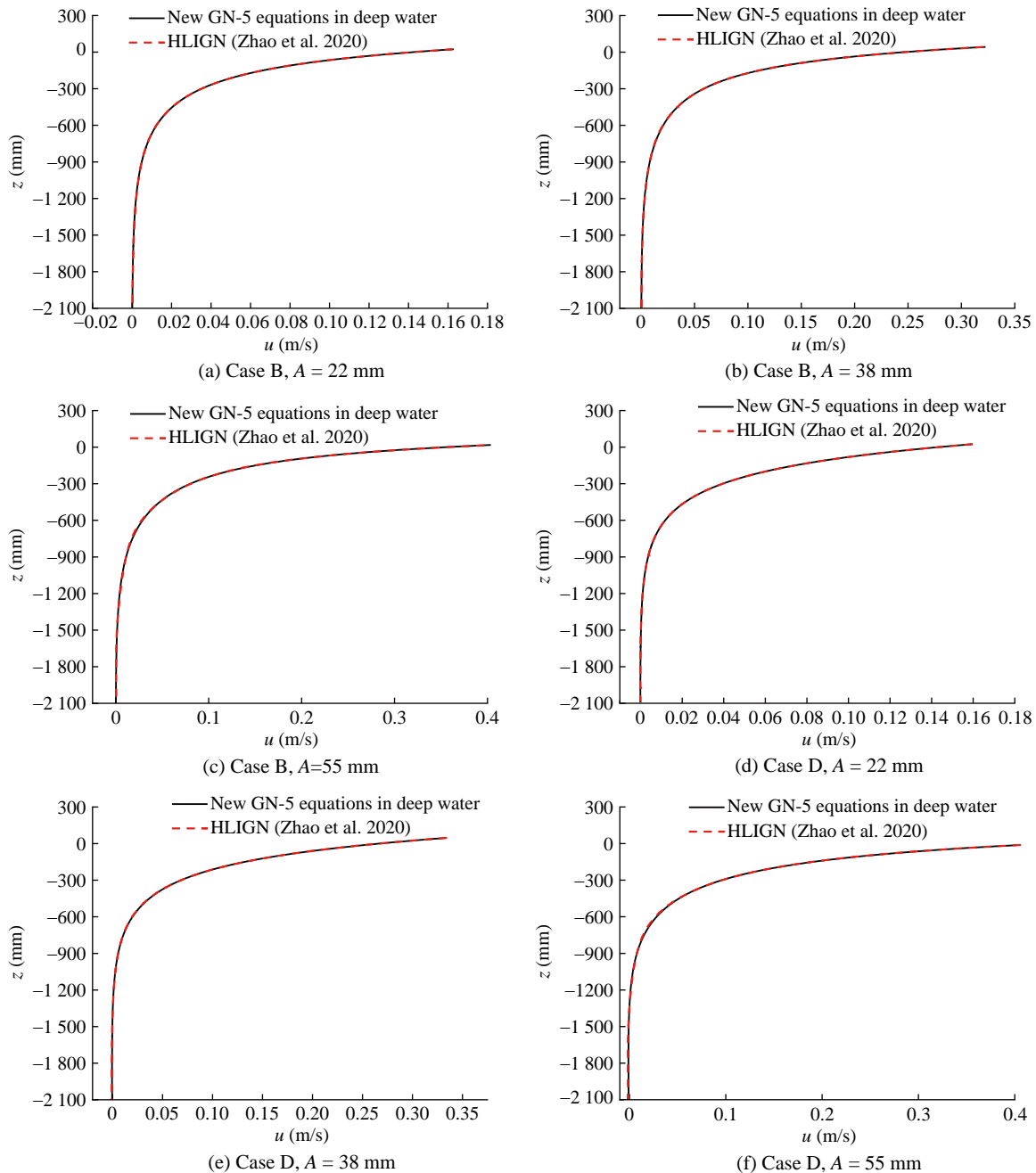


Figure 6 Horizontal velocity distribution beneath the focused crest of Cases B and D

−0.7 m is not zero, as shown in Figure 6, which explains why the wave flume experimental data (Baldock et al. 1996) with 0.7 m water depth are not true deep water-focused wave results. It can also be seen that the horizontal velocity decreases to zero at $z = -2.1$ m. As a result, 2.1 m water depth corresponds to the deep water results for Cases B and D. The good agreement between these results, as shown in Figure 6, also demonstrates that the new velocity assumption in Eq. (9) is quite accurate for deep water waves.

5 Conclusions

In this paper, new three-dimensional deep water GN equations are derived using a new velocity assumption, and the linear dispersion relations of GN equations are studied. Furthermore, the current GN-5 equations with the new exponential shape functions are used to simulate focused waves in deep water, and the results are compared to other deep water numerical results (Zhao et al. 2020). The good agreement between these two numerical results for focused wave profiles indicates that the new deep water GN equations are accurate in time domain wave simulation. In addition, the new exponential velocity assumption is reasonable, as evidenced by a good agreement in horizontal velocity distribution along the water depth. Therefore, these new GN equations are expected to have a high potential for simulating strongly nonlinear short-crest waves in the deep ocean.

Open Access This article is licensed under a Creative Commons Attribution 4.0 International License, which permits use, sharing, adaptation, distribution and reproduction in any medium or format, as long as you give appropriate credit to the original author(s) and the source, provide a link to the Creative Commons licence, and indicate if changes were made. The images or other third party material in this article are included in the article's Creative Commons licence, unless indicated otherwise in a credit line to the material. If material is not included in the article's Creative Commons licence and your intended use is not permitted by statutory regulation or exceeds the permitted use, you will need to obtain permission directly from the copyright holder. To view a copy of this licence, visit <http://creativecommons.org/licenses/by/4.0/>.

References

- Baldock TE, Swan C, Taylor PH (1996) A laboratory study of nonlinear surface waves on water. *Philosophical Transactions of the Royal Society of London. Series A: Mathematical, Physical and Engineering Sciences* 354(1707): 649–676. DOI: 10.1098/rsta.1996.0022
- Demirbilek Z, Webster WC (1992) Application of the Green–Naghdi theory of fluid sheets to shallow-water wave problems. Report 1. Model Development. Coastal Engineering Research Center,

- Vicksburg, Technical Report No. CERC-92-11. <https://doi.org/10.1017/S0022112086000630>
- Ertekin RC, Webster WC, Wehausen JV (1986) Waves caused by a moving disturbance in a shallow channel of finite width. *J Fluid Mech* 169: 275–292. <https://doi.org/10.1017/S0022112086000630>
- Green AE, Laws N, Naghdi PM (1974) On the theory of water waves. *Proc R Soc Lond A Math Phys Sci* 338: 43–55. <https://doi.org/10.1098/rspa.1974.0072>
- Green AE, Naghdi PM (1976) Directed fluid sheets. *Proc R Soc Lond A Math Phys Sci* 347: 447–473. <https://doi.org/10.1098/rspa.1976.0011>
- Hayatdavoodi M, Treichel K, Ertekin RC (2019) Parametric study of nonlinear wave loads on submerged decks in shallow water. *Journal of Fluids and Structures* 86: 266–289. <https://doi.org/10.1016/j.jfluidstructs.2019.02.016>
- Hayatdavoodi M, Liu J, Ertekin RC (2022) Bore impact on decks of coastal structures. *Journal of Waterway, Port, Coastal, and Ocean Engineering* 148(2): 04021051. DOI: 10.1061/(ASCE)WW.1943-5460.0000696
- Hayatdavoodi M, Ertekin RC (2022) On some nonlinear wave diffraction and refraction solutions in shallow waters. *International Conference on Offshore Mechanics and Arctic Engineering*, Vol. 85895, V05AT06A004
- Kostikov VK, Hayatdavoodi M, Ertekin RC (2022) Drift of elastic floating ice sheets by waves and current: Multiple sheets. *Physics of Fluids* 34(5): 057113. DOI: 10.1063/5.0091538
- Liu J, Hayatdavoodi M, Ertekin RC (2019) Bore pressure on horizontal and vertical surfaces. *International Conference on Offshore Mechanics and Arctic Engineering*, Vol. 58844, V07AT06A008. DOI: 10.1115/OMAE2019-96013
- Liu J, Hayatdavoodi M, Ertekin RC (2020) On bore dynamics and pressure: RANS, Green–Naghdi, and Saint-Venant equations. *Journal of Offshore Mechanics and Arctic Engineering* 142(2): 021902. DOI: 10.1115/1.4044988
- Wang Z, Zhao BB, Duan WY, Ertekin RC, Hayatdavoodi M, Zhang TY (2020) On solitary wave in nonuniform shear currents. *Journal of Hydrodynamics* 32(4): 800–805. DOI: 10.1007/s42241-020-0051-z
- Webster WC, Kim DY (1991) The dispersion of large-amplitude gravity waves in deep water. *Water Waves*, 397–416. <https://trid.trb.org/view/439579>
- Webster WC, Duan WY, Zhao BB (2011) Green–Naghdi theory, part A: Green–Naghdi (GN) equations for shallow water waves. *Journal of Marine Science and Application* 10(3): 253–258. DOI: 10.1007/s11804-011-1066-1
- Webster WC, Zhao BB (2018) The development of a high-accuracy, broadband, Green–Naghdi model for steep, deep-water ocean waves. *Journal of Ocean Engineering and Marine Energy* 4(4): 273–291. DOI: 10.1007/s40722-018-0122-1
- Zhao BB, Duan WY, Ertekin RC (2014) Application of higher-level GN theory to some wave transformation problems. *Coastal Engineering* 83: 177–189. DOI: 10.1016/j.coastaleng.2013.10.010
- Zhao BB, Zheng K, Duan WY, Ertekin RC, Shao YL (2020) Time domain simulation of focused waves by High-Level Irrotational Green–Naghdi equations and Harmonic Polynomial Cell method. *European Journal of Mechanics-B/Fluids* 82: 83–92. DOI: 10.1016/j.euromechflu.2020.02.006
- Zheng K, Zhao BB, Duan WY, Ertekin RC, Chen XB (2016) Simulation of evolution of gravity wave groups with moderate steepness. *Ocean Modelling* 98: 1–11. DOI: 10.1016/j.ocemod.2015.12.003